VOL. 17, NO. 5, SEPT.-OCT. 1980 J. SPACECRAFT 447

ARTICLE NO. 79-1293R

A80-078

Pulsed Plasma Thruster Backflow Characteristics

20007
60004
60007

L. K. Rudolph,* L. C. Pless,† and K. G. Harstad‡
Jet Propulsion Laboratory, California Institute of Technology, Pasadena, Calif.

The exhaust plume of a millipound pulsed plasma thruster has been investigated using a unique vacuum facility with cryogenically cooled low-backscatter chamber walls. The mass flux distribution of the plume was determined, with emphasis on the region upstream of the thruster. Measurements of the plume material scattered from the chamber walls were used with articulated collimator-quartz crystal microbalance measurements of the total flux to estimate the upstream flux originating in the plume. This flux was found to be of order 10^{-10} g-cm^{-2}-pulse^{-1} and to vary approximately with the inverse square of the radius. Measurements indicate the directed plume is essentially axisymmetric with a slight elongation in the direction parallel to the interelectrode gap. This downstream flux decreases with radius along an approximate Gaussian profile with 90% of the plume confined to a 40 deg half-angle cone.

Introduction

PULSED plasma thrusters (PPT's) using solid teflon propellant have a flight-demonstrated simplicity and reliability[1] and are of increasing interest for future flight applications. Earlier versions of this thruster have relatively low values of impulse bit and total impulse, and hence, are limited to applications such as east-west stationkeeping and fine attitude control.[2] To extend the capabilities of the PPT to longer duration missions and larger spacecraft, a one millipound average thrust PPT is currently in the advanced stages of development.[3] This thruster has an impulse bit of 22.2 mN-s, roughly 50 times larger than earlier versions, and a total impulse of 310,800 N-s, roughly 10 times larger than earlier versions. In addition, its specific impulse, propellant flow rate, efficiency, and power are also significantly larger. Applications envisioned for this millipound thruster include north-south stationkeeping, orbital acquisition and maneuvering, and large structure attitude control.

The flight experience of the earlier PPT's has shown that the exhaust plume of these smaller thrusters has a negligible effect on spacecraft surfaces.[4] The exhaust plume of the one millipound thruster is of potentially greater concern, primarily due to its higher energy and greater mass per pulse. In addition, longer mission durations and ever more sensitive spacecraft instrumentation will aggravate any plume contamination that may exist. Previous studies have been conducted to assess the effect of the one millipound PPT plume on spacecraft surfaces by directly measuring the plume flux impinging on a spacecraft upstream of the thrust exhaust plane.[5] Unfortunately, accurate results have been masked by a backscattered flux of particles reflected and eroded from the test facility vacuum chamber walls. In order to minimize this effect and develop a more accurate measure of the plume-spacecraft interaction, a study has been carried out using a special molecular sink (MOLSINK) vacuum facility.[6,7] This facility has a gaseous helium cooled anechoic-type liner (MOLTRAP), designed to minimize any plume-wall backscatter and provide an environment in which accurate plume-spacecraft interaction measurements can be made.

Following a brief description of the experimental equipment used for this study, this paper will discuss the results of a series of investigations of the PPT plume and its interaction with the MOLTRAP wall. Measurements will be shown which indicate the plume is essentially axisymmetric with a mass flux which drops to 10% of its centerline value at a location 40 deg off the thruster axis. When operated in the MOLSINK facility, this plume behavior gives a wall backscatter distribution essentially confined to a region within the intersection of the wall and the 40 deg half-angle plume boundary. A method of measuring the plume backflow using articulated collimator-quartz crystal microbalances (QCM's) will be described and the results of the measurements at various axial, radial, and azimuthal locations will be analyzed.

Thruster and Diagnostic Facilities

The pulsed-plasma thruster under investigation in this study has been described in Refs. 3 and 5. The thruster was enclosed in an electrically isolated aluminum box, approximately 0.4 m on a side. To prevent its oil-filled discharge capacitors from freezing, the interior of this box was heated to 20-26°C at all times. To relieve the heat loading on the MOLSINK cryogenic pumping system, the thruster pulse rate was dropped from its design value of approximately 5 s/pulse to between 20 and 40 s/pulse. To check for proper thruster operation, a Rogowski coil on one of the discharge capacitor leads was used to monitor the thruster current.

The MOLSINK vacuum facility was designed to provide an ideal simulation of the vacuum and cold sink of outer space.[8] It consists of an ultrahigh vacuum chamber (10^{-12} Torr) with a liquid nitrogen (LN_2) cooled liner to provide a thermal isolation barrier. This liner encloses a 2.75 m effective outer diameter molecular trap (MOLTRAP) which has black anodized aluminum anechoic walls cooled by a manifold of tubes carrying gaseous helium at 10-15 K. This large cryogenic pumping area (186 m^2) is particularly useful for thruster plume studies, due to its high pumping rate and minimal backscatter.

Figure 1 shows a cross-sectional schematic of the MOLSINK facility with the PPT in place. The thruster is installed by hanging it from a support shaft reaching through the upper access port and an opening in the MOLTRAP. This support shaft may be externally rotated, allowing the thruster to turn about its axis to provide for testing the azimuthal plume variation. The thruster is fired downward from a nozzle location slightly above the center of the MOLTRAP to provide maximum thermal isolation from the MOLTRAP walls while leaving room for the experimental diagnostics.

Presented as Paper 79-1293 at the AIAA/SAE/ASME 15th Joint Propulsion Conference, Las Vegas, Nev., June 18-20, 1979; submitted Sept. 25, 1979; revision received March 17, 1980.

Index categories: Electric and Advanced Propulsion; Environmental Effects; Jets, Wakes, and Viscid-Inviscid Flow Interactions.

*Senior Engineer. Member AIAA.
†Member, Technical Staff.
‡Member, Technical Staff.

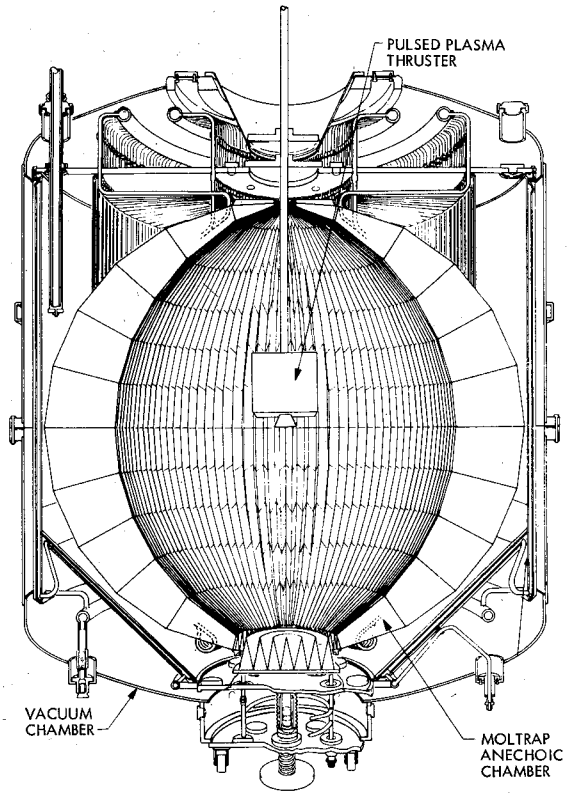

Fig. 1 MOLSINK vacuum chamber.

Doublet temperature-compensated QCM's were used to measure the mass flux from the PPT plume.[9] Briefly, two crystal-controlled oscillators are formed with two electrodes on the same side of a natural quartz blank. An electronic circuit extracts the difference frequency between these two oscillators. Mass is allowed to deposit on one electrode, slowing its oscillation and increasing the difference frequency, which is measured and related to the mass deposition through a calibration constant. To insure that the PPT plume mass flux that impinges on the QCM is actually deposited on the QCM electrode, the entire QCM was cooled to LN_2 temperature. Due to this temperature requirement and to insure that the QCM's would survive in the electromagnetically noisy PPT discharge environment, these QCM's were designed and built specifically for this program.

The accuracy of a particular QCM measurement depends on several factors which can be split into two broad areas.[7] The first area includes factors which describe the relation between the mass flux at a certain location and the actual collected mass when a QCM is at this location. These factors include considerations of the particle optics to the sensing crystal (i.e., collimator design and leakage), spurious mass accumulation (due to the vacuum tank environmental pressure and the pulsed thruster operation), and the accommodation coefficient of the collecting surface. The second area includes factors which relate the accumulated mass to the measured output frequency shift. These factors include the QCM temperature sensitivity and electronic stability, the value of the calibration constant, and the calculation of the frequency shift vs time. The total error in the QCM flux measurements is, on the average, about ±20%; however, for selected data it can be as high as a factor of 2.5, due to potential spurious mass accumulation.

Measurements of the total plume-wall backscatter were made using QCM's facing the MOLTRAP wall about 10 cm away and mounted on brackets designed to minimally interfere with the plume. As shown in Fig. 2, these QCM's were mounted at locations corresponding to angles of 45, 60, and 75 deg off the thruster axis from the MOLSINK center. Also shown in Fig. 2 is the articulated collimator QCM array

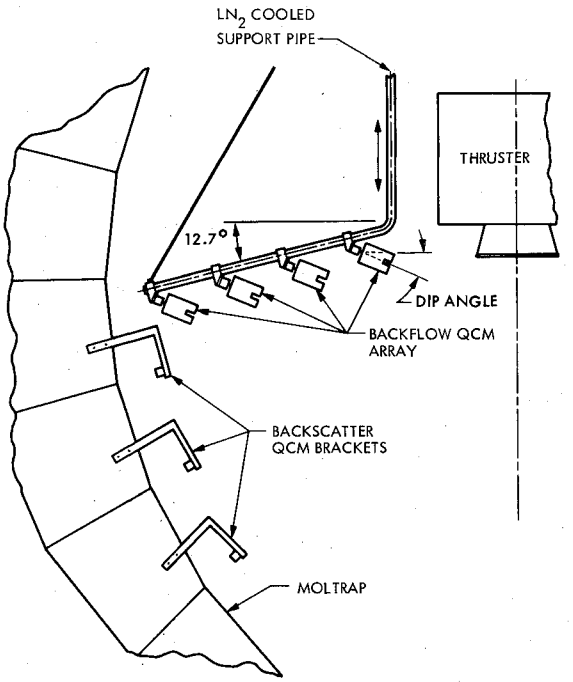

Fig. 2 Plume backflow test assembly.

designed to measure the PPT plume backflow in the presence of the plume-wall backscatter. Eight QCM's were mounted in pairs to provide redundancy in case of failure. The pairs occupy four rows, 38 cm, 54 cm, 70 cm, and 86 cm from the thruster axis, respectively. The QCM's look toward the thruster axis through individual collimators designed to limit each QCM's observed volume to a planar slice of the PPT plume. The observed slice intercepts the thruster axis at a "dip" angle which can be varied from 0 to 60 deg by rotating the collimator about a horizontal axis located on the QCM surface and perpendicular to a radial line from the thruster axis. When the dip angle is set at 0 deg, the observed slice is perpendicular to the thruster axis. The collimator is designed to limit the thickness of this slice to an effective aperture angle of 5.7 deg in the axial direction (at 0 deg dip angle) and the width to an angle of 100 deg in the radial direction. In order to prevent the QCM's mounted on the inner radii from interfering with those on the outer radii, the QCM mount is tilted downward by 12.7 deg, such that each pair of QCM's is displaced axially downstream 3.6 cm from the next closest pair. The entire array can be raised or lowered to measure the plume backflow at various axial positions.

Plume Studies

To assist in the development of a plume backflow measuring technique, which is unaffected by the plume backscatter from the vacuum facility walls, some preliminary studies of the character of the main PPT plume downstream of the nozzle were carried out. These studies were required in order to determine the mass flux profile in the plume, and hence, the distribution of mass impinging on and possibly scattering from the vacuum facility walls. Due to the complexity and expense of operating the MOLSINK facility and because the results of these particular studies are unaffected by the facility, the experiments were carried out in an alternate vacuum facility, 2.3 m in diameter and 4.6 m long, with an LN_2-cooled liner and an ultimate vacuum of approximately 10^{-6} Torr.

The exit orifice of the PPT exhaust nozzle is an 11.5 × 16.5 cm rectangle. This azimuthally nonsymmetric shape implies that the exhaust plume may also be nonsymmetric, thus requiring any plume measurement to be made at various azimuthal as well as radial locations. Recent studies indicate that 40 cm downstream of the nozzle exit plane, the PPT

plume is elliptical in cross section with an aspect ratio of approximately 1.2.[10] These results suggest that at greater downstream axial locations, the plume may approach azimuthal symmetry. To verify this possibility, a 1 m square sheet of 1 mil thick mylar coated with a layer of aluminum was placed 76 cm downstream of the PPT nozzle exit plane on a frame supporting its top and bottom edges. A 38 cm diameter hole was cut in the center of this sheet to permit the central core of the PPT plume to escape without damaging the fragile mylar. The thruster was discharged approximately 12,000 times, after which the target was examined for signs of plume deposition or erosion. A series of varicolored concentric rings was observed, surrounding the central hole in the target and extending out to a radius of 65 cm, corresponding to an angle from the thruster axis of 40 deg. Each ring is circular with only a slight bump at an azimuthal angle corresponding to the location of the PPT cathode; hence, for locations beyond 76 cm downstream of the nozzle, the plume is essentially axisymmetric. In the MOLSINK facility, the thruster is roughly 1.5 m from the wall; hence, the plume wall impingement and subsequent backscatter should also be axisymmetric.

Previous attempts to determine the radial distribution of the PPT plume mass flux profile with a single QCM have met with little success because the plume erodes the QCM collecting surface rather than depositing on it.[5] To accurately measure this plume mass flux profile, a special double QCM probe was designed and is sketched in Fig. 3. It consists of a shielded container with an aperture designed to direct incoming mass to QCM 1, placed at an angle of 45 deg with respect to the incoming axis. Some of the material which reflects or erodes from QCM 1 is captured by QCM 2, placed normal to the incoming axis on the optical path from QCM 1. This probe was mounted on a movable support 74 cm downstream of the PPT nozzle exit plane, and swept over radius out to a distance of 75 cm from the thruster axis. The observed data is shown in Fig. 4. For radii less than 45 cm, QCM 1 indicates a net mass loss or erosion from its collecting surface, as is consistent with previous studies.[5] QCM 2 shows a net mass accumulation of roughly one third the magnitude of the signal from QCM 1.

The data of Fig. 4 can be reduced to a total plume mass flux profile through the following analysis, which presumes that a negligible amount of material is reflected or eroded from QCM 2, and that the fraction of material eroded or reflected from QCM 1, which is collected by QCM 2, is independent of radius. The net signal output S_1 of QCM 1 is equal to the rate of material deposited on the crystal sensor. This rate is equal to the axial component of the local plume mass flux $\dot{m}$, less the amounts reflected and ablated, $\dot{m}_r$, from the QCM surface:

$$S_1 = \dot{m} \cos 45 \text{ deg} - \dot{m}_r \tag{1}$$

The cos 45 deg is required to correct for the angle between the incoming axis and the QCM collecting surface normal. The reflected and ablated mass flux leaves the surface of QCM 1 in some unknown distribution about the QCM surface normal. Some fraction B of this mass flux impinges on and is collected by QCM 2. Thus, the signal output S_2 of QCM 2 is

$$S_2 = B\dot{m}_r \tag{2}$$

The plume mass flux can be found by eliminating the reflected and ablated mass flux from Eqs. (1) and (2):

$$\dot{m} = (S_1 + S_2/B)\, 1/\cos 45 \text{ deg} \tag{3}$$

The values of S_1 and S_2 can be measured locally to give a local value of $\dot{m}$, provided B is known. This constant can be found through a calculation of the total mass flow rate $\dot{m}_T$ from the thruster discharge as follows.

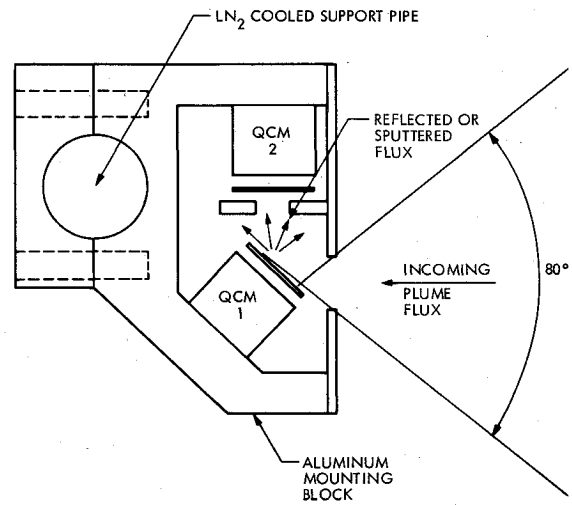

Fig. 3 Double QCM probe.

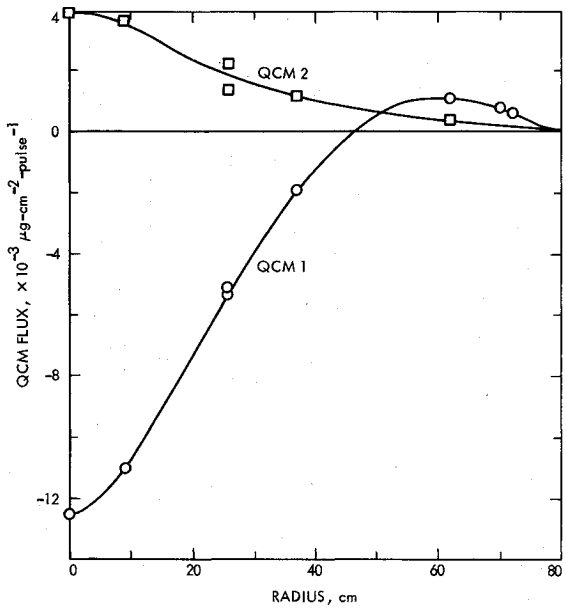

Fig. 4 QCM flux profiles.

The total mass flux over the entire plume cross section is given by

$$\dot{m}_T = \int_A \dot{m} \mathrm{d}A \tag{4}$$

where dA is the differential cross-sectional area element normal to the thruster axis. Substituting into Eq. (3):

$$\dot{m}_T = \left\{ \int_A S_1 \mathrm{d}A + \int_A \frac{S_2}{B} \mathrm{d}A \right\} \frac{1}{\cos 45 \text{ deg}} \tag{5}$$

Under the assumption that B is independent of radius, Eq. (5) can be solved for B as follows:

$$B = \left(\dot{m}_T \cos 45 \text{ deg} - \int_A S_1 \mathrm{d}A \right) \Big/ \int_A S_2 \mathrm{d}A \tag{6}$$

The total mass flow rate is known to be 1.56 mg/pulse; thus measurements of S_1 and S_2 vs radius can be used to experimentally evaluate B. Once known, B can be substituted along with local values of S_1 and S_2 into Eq. (3) to give the local axial plume mass flux. The resulting mass flux profile is

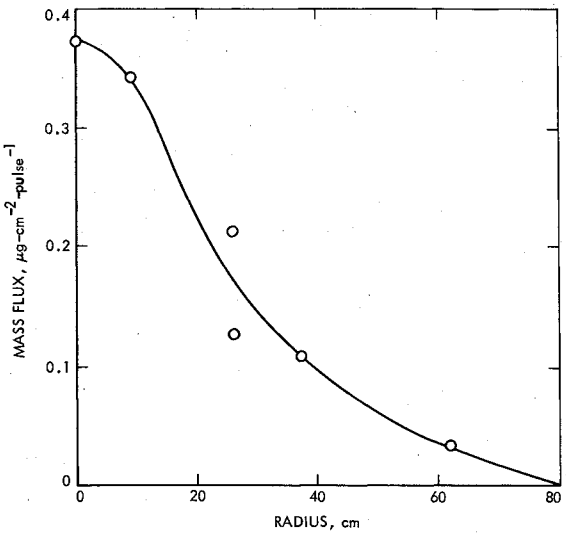

Fig. 5 PPT plume mass flux profile.

shown in Fig. 5. As can be seen, this profile follows an approximate Gaussian shape with a half-width of about 28 cm. At a radius of 60 cm, corresponding to an angle from the thruster axis of 40 deg, the plume flux has dropped to less than 10% of its centerline value, as is consistent with the indications of the aluminized mylar target results.

PPT Plume Wall Backscatter

The results of the previous PPT plume studies indicate that any primary plume backscatter from the MOLTRAP walls will occur on the wall areas within a 40 deg half-angle cone centered on the thruster axis. Furthermore, since the MOLTRAP is symmetric about this axis, this backscatter should also be axisymmetric.

To determine the magnitude of the wall backscatter, a test was run using the three wall-mounted QCM's described previously and shown in Fig. 2. Presuming a cosine scattering distribution, the results of these measurements were converted into source intensities in units of micrograms scattered per pulse per unit wall area into a unit solid angle, and are shown in Fig. 6 vs the angle Ψ measured from the plume axis and originating at the center of the MOLSINK, approximately in the nozzle exit plane. Also shown in this figure is the flux intensity at an angle of 0 deg, measured in a test described in Ref. 6 and representing the backscatter from only the first wall-plume interaction. Because this intensity does not include contributions from the interactions which follow the first, it is, at best, a lower estimate of the total backscatter at this location. Even so, it is still too high for accurate plume backflow measurements with ordinary uncollimated QCM's. The data of Fig. 6, excluding the data at $\Psi = 0$ deg, fit an exponential curve of the form

$$I_B = 9.78 \times 10^{-3} e^{-\Psi/17\,\text{deg}} \tag{7}$$

Because of this exponential dropoff with angle, a method using collimated QCM's to indirectly measure the plume backflow was developed. These collimated QCM's are designed to observe only those sections of the wall at angles greater than 40 deg where the backscatter flux is negligible.

Plume Backflow Analysis

Using the collimated QCM array described earlier and shown in Fig. 2, the plume backflow was measured. The measurements were made at three array axial locations, such that the array QCM pair closest to the thruster (at a radius of 30 cm) was 11.1 cm upstream, 2.54 cm downstream, and 30.5 cm downstream of the PPT nozzle exit plane. At each axial location, data were recorded over a range of dip angles from 0

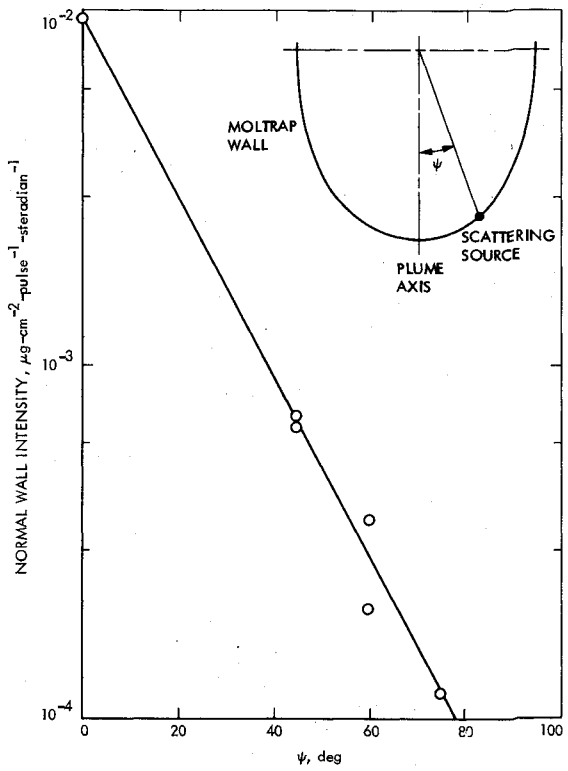

Fig. 6 Total backscatter distribution.

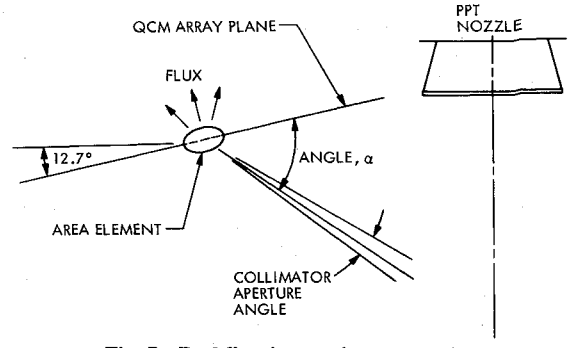

Fig. 7 Backflow integration schematic.

to 60 deg to eventually be summed in order to determine the total plume backflow flux vs position. In order to insure that the measured axisymmetry in the main PPT plume also exists in the plume backflow distribution, the QCM array data at the 11.1 cm upstream axial position were taken at two thruster rotational positions, displaced by 90 deg. These data were found to be identical within experimental error, over the entire range of collimator dip angle, thus confirming the expected axisymmetry of the PPT plume backflow.

To give useful results, the geometric effects of the collimator must be removed from the QCM fluxes at each position. The QCM flux results from an accumulation of particles from the solid angle defined by the aperture of the collimator, and an area defined by the collector opening in the back of the collimator, just in front of the QCM collecting surface (see Fig. 7). The QCM mass accumulation rate can be converted to an intensity by dividing it by the collimator solid angle and the collector area. The total mass flux through a reference plane may then be estimated by integrating the product of the intensity and the cosine of the angle between the intensity direction and the reference plane normal, over the total span of intensity directions. Application of this procedure is discussed in the following.

Since it has been concluded that scattering from the plume is axisymmetric, the average signals from the side-by-side

mounted QCM pairs are used in the analysis. These signals represent the sum of the wall backscatter and the plume backflow fluxes which reach the QCM collecting surface. Since the plume backflow flux is desired, the wall backscatter flux must be subtracted from these signals. To calculate the backscatter corrections to the QCM signals, the previously described results of the wall backscatter measurements are used. In this calculation, all the particles leaving an effective wall source (Fig. 6) in the direction of a given QCM collimator are assumed to reach it, with no attenuation. A particular source element may be partially or totally screened from the collector opening by the aperture slit. This effect is complex; hence, a computer analysis was required to calculate the total signal by summing over many small discrete wall elements. The quantity summed is the product of the appropriate area, solid angle, direction cosine, and normal intensity. For dip angles greater than 40 deg, the correction term is considerably larger than the QCM signal, indicating that considerable attenuation of backscattered wall flux (by nearly an order of magnitude) must occur, and that collisional effects in the plume are important. Rather than attempting to account for these collisional effects, the calculated backscatter correction term is simply used as an upper bound indicator to show which QCM signals have potentially large wall backscatter components. Those QCM signals whose calculated corrections are comparable to or greater than the signal itself will be ignored. These ignored signals occur for dip angles greater than some maximum value α_{max}, which depends on the particular QCM location.

Since backflow variations transverse to the plume are not determined by use of the slit collimator geometry, only variations with respect to the dip angle can be calculated. Backflow partial fluxes through a plane parallel to the QCM array mounting are estimated. The QCM mount tilts at an angle of 12.7 deg plus the dip angle, and sinα is equal to the cosine of the angle from the normal. The backflow from the plume volume, bounded by dip angles of 0 and $\alpha \leq \alpha_{max}$, is referred to as the partial flux and is given by

$$F(\alpha) = \int_0^{\alpha} I(\alpha) \sin\alpha d\alpha \tag{8}$$

where $I(\alpha)$ is th plume backflow flux intensity at a given dip angle. The uncorrected QCM signal, $I_{QCM}\sin\alpha$, and the same signal with the backscatter subtracted, $(I_{QCM} - I_{Backscatter})\sin\alpha$, are shown vs dip angle in Fig. 8. From this figure, α_{max} can be seen to be approximately 45 deg. The net backflow integrand used in Eq. (8) represents an average between the previous two curves out to α_{max} and is also shown in Fig. 8. Partial fluxes for $\alpha = \alpha_{max}$ and the associated values of α_{max} are listed in Table 1. Values were obtained by graphical integration.

In the range $25 \leq \alpha \leq 50$ deg, the partial flux varies approximately as α^2 for those cases of larger α_{max}. This behavior suggests that the partial integrals for small α_{max} may be extrapolated to larger α_{max} values. A least-square curve fit of the form

$$F = k(\alpha_{max})^2 r^{-p} \tag{9}$$

with axial variations removed through division by the $r = 54$ cm values gives $p \simeq 2$. Using $p = 2$, the coefficient k may be estimated as a function of axial position. For α in degrees, results are presented in Table 2.

For each position, the rms error is slightly below 40%. The rough curve fit gives consistently high fluxes at $r = 70$ cm and consistently low fluxes at $r = 86$ cm. Using the above k to remove the mean axial dependence of the partial fluxes, and using the assumed α^2 variation to shift the fluxes to $\alpha_{max} = 50$ deg values, the radial dependence and data scatter are shown in Fig. 9. Although another radial dependence could possibly give a slightly better fit, it is felt that inaccuracies in the data and the extrapolation procedure do not make it necessary or desirable.

Table 1 Plume backflow results, $\times 10^{-4}$ μg-cm^{-2}-pulse^{-1} (α_{max}, deg)

Array position	QCM radius, cm			
	38	54	70	86
30.5 cm downstream	54 (54)	15 (54)	3.4 (36)	5.1 (36)
2.5 cm downstream	4.2 (44)	1.2 (34)	0.12 (22)	0.33 (26)
11.1 cm upstream	6.3 (54)	4.4 (45)	0.83 (30)	1.4 (36)

Table 2 Partial flux axial coefficient k, $\times 10^{-4}$ μg-pulse^{-1}-deg^{-2}

Array position	k	Standard deviation
30.4 cm downstream	20.9	8.2
2.54 cm downstream	2.75	1.0
11.1 cm upstream	5.49	2.1

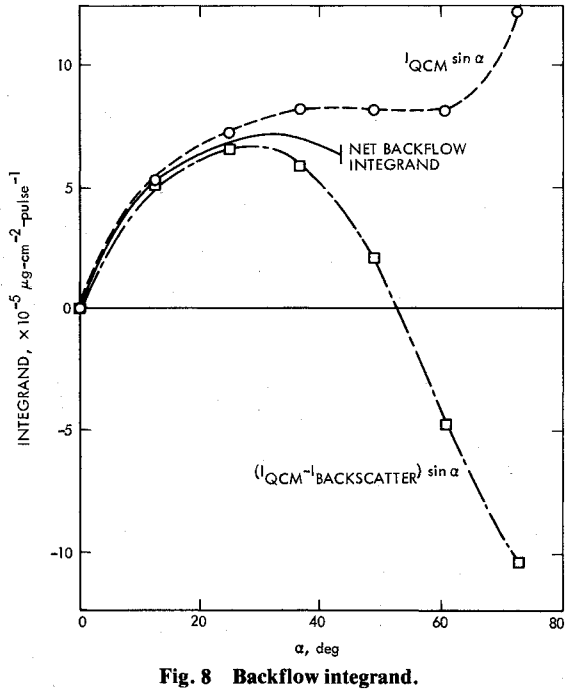

Fig. 8 Backflow integrand.

The plume expansion angle is approximately 40 deg, thus the dip angle parallel to the plume boundary is roughly 140 deg. At this angle, since there is little if any plume mass, the backflow should approach zero. Furthermore, for dip angles which observe volumes well downstream of the thruster; i.e., for $\alpha = 50$ deg or more, it may be expected that the backflow would drop to small values. Backflow intensity plots similar to Fig. 8 support this possibility and suggest that the total backflow flux may be estimated by multiplying the partial backflow fluxes for $\alpha = 50$ deg by a factor of two or three.

To place these measured backflow fluxes in context with the backflow fluxes of other thruster types, a comparison was made between these fluxes and those of an 8-cm ion bombardment thruster. This particular ion thruster was developed for applications similar to those of the pulsed plasma thruster, including stationkeeping and attitude control of orbiting

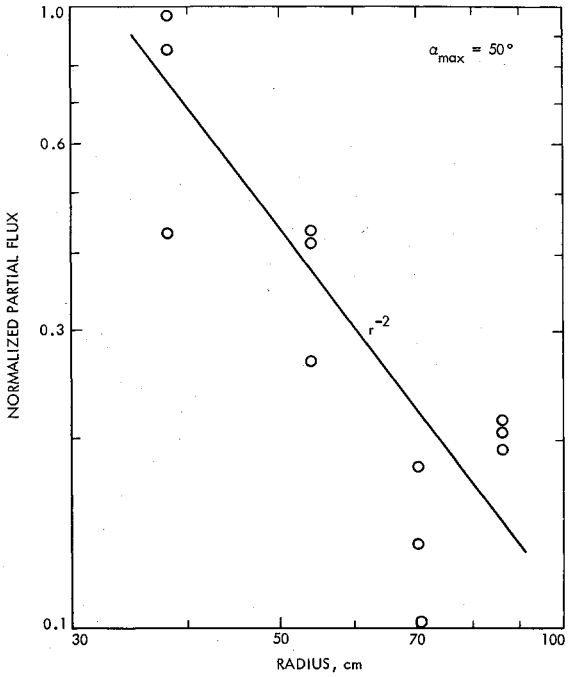

Fig. 9 Backflow flux radial profile.

spacecraft. This ion thruster has a thrust of one millipound, as does the PPT; however, its specific impulse is approximately 60% higher and its mass flow rate is 40% lower than the PPT. The total backflow from the plume of this ion thruster was estimated by summing the contributions from both the mercury propellant and molybdenum sputtered from the grids,[11] for locations identical to those where the PPT backflow measurements were made. The backflow flux from the PPT, as shown in Table 2, was corrected for the nominal pulse rate of 0.2 pps and was found to be identical, within experimental error, to that found for the ion thruster.

Conclusion

The one millipound pulsed plasma thruster (PPT) is being developed for applications requiring larger impulse bits and larger total impulses than previously existed in such thrusters. This increased capability is expected to be accompanied by an increase in the plume contamination levels upstream of the thruster. Concern for this possibility has led to the necessity of measuring this contamination. Previous measurements of the PPT plume backflow have been obscured by plume-vacuum facility backscatter; hence, this problem was of particular concern in the current work. To minimize this potential problem and to develop an accurate measure of the one millipound PPT backflow, the MOLSINK vacuum facility was chosen for these tests, since it was specifically designed to provide an environment free of tank wall effects.

Prior to the MOLSINK backflow measurements, several preliminary tests were performed to determine the relevant PPT plume characteristics and wall backscatter magnitudes. Investigations of the plume mass flux profile indicate that it is essentially axisymmetric for locations over 76 cm downstream of the nozzle and that it follows a radial profile that is approximately Gaussian with 90% of the flux confined to a 40 deg half-angle cone centered on the thruster axis. Based on these observations, measurements of the plume-MOLSINK wall backscatter were made which led to the development of an approximate analytic expression for the backscatter mass flux intensity. This expression was then used in the plume backflow measurements to remove the effect of wall backscatter.

Using an articulated collimator array of eight QCM's, backflow measurements were made of a volume from 38 out to 86 cm in radius, and between 11.1 cm upstream and 30.5 cm downstream of the PPT nozzle. These measurements indicate the total plume backflow flux is of order 10^{-10} g-cm^{-2}-pulse^{-1} and falls off approximately with the inverse square of the radius. The accuracy of these measurements depends not only on the accuracy of the QCM signals, but also on the errors induced in the reduction of these signals to the final backflow values. Although a precise error analysis is not possible, estimates place the total backflow flux error at about a factor of 5 or less.

A comparison between the measured backflows of the PPT and the 8 cm ion bombardment thruster was made in order to develop a baseline estimate of whether or not the measured PPT backflow is too large for the envisioned thruster applications.[11] Both thrusters have an average thrust of about 4.4 mN and are designed for similar uses. The comparison indicated that the total mercury and molybdenum backflow flux from the 8 cm ion thruster is of the same order as the measured PPT flux. This implies that the PPT backflow is satisfactorily low; however, questions remain on the relative effects of the PPT backflow effluents on sensitive spacecraft surfaces. Until these questions are answered, it will remain difficult to determine the necessary upper bounds on the tolerable backflow from this thruster.

Acknowledgments

The research described in this paper represents work carried out at the Jet Propulsion Laboratory, California Institute of Technology and sponsored by the Air Force Rocket Propulsion Laboratory through an agreement with NASA.

References

[1] MacLellan, D.C., MacDonald, H.A., Waldon, P., and Sherman, H., "Lincoln Experimental Satellites 5 and 6," AIAA Paper 70-494, AIAA Third Communications Satellite Systems Conference, Los Angeles, Calif., April 1970.

[2] Rosen, S.G., "Colloid and Pulsed Plasma Thrusters for Spacecraft Propulsion," AIAA Paper 73-1254, AIAA/SAE 9th Propulsion Conference, Las Vegas, Nev., Nov. 1973.

[3] Guman, W.J. and Palumbo, D.J., "Pulsed Plasma Propulsion System for North-South Stationkeeping," AIAA Paper 76-999, AIAA International Electric Propulsion Conference, Key Biscayne, Fla., Nov. 1976.

[4] Lyon, W.C., "Thruster Exhaust Effects upon Spacecraft," AIAA Paper 70-1143, AIAA 8th Electric Propulsion Conference, Stanford, Calif., Aug.-Sept. 1970.

[5] Guman, W.J. and Begun, M., "Pulsed Plasma Plume Studies," Air Force Rocket Propulsion Lab. TR-77-2, March 1977.

[6] Pless, L.C., Rudolph, L.K., and Fitzgerald, D.J., "Plume Characteristics of a One-Millipound Solid Teflon Pulsed Plasma Thruster-Phase I Final Report," Air Force Rocket Propulsion Lab., TR-78-63, Oct. 1978.

[7] Rudolph, L.K., Pless, L.C., and Harstad, K.G., "Plume Characterization of a One-Millipound Solid Teflon Pulsed Plasma Thruster-Phase II Final Report," Air Force Rocket Propulsion Lab., TR-79-60, Sept. 1979.

[8] Stephens, J.B., "Space Molecular Sink Facility," 2nd Aerospace Mechanisms Symposium, May 1967.

[9] Holland, J. (ed.), *Thin Film Microelectronics,* John Wiley & Sons, Inc., New York, 1965.

[10] Palumbo, D.J. and Begun, M., "Experimental and Theoretical Analysis of Pulsed Plasma Exhaust Plumes," Air Force Office of Scientific Research, TR-78-1242, July 1978.

[11] Komatsu, G.K., Sellen, J.M. Jr., and Zafran, S., "Ion Beam Plume and Efflux Measurements of an 8-cm Mercury Ion Thruster," AIAA Paper 78-676, AIAA/DGLR 13th International Electric Propulsion Conference, April 1978.